Time dependent quantum dynamical study of laser induced current switching in graphene

Satofumi Souma[†], Takashi Akiyama, Kenji Sasaoka* and Matsuto Ogawa

Department of Electrical and Electronic Engineering, Kobe University, Kobe 657-8501, Japan

[†]email: ssouma@harbor.kobe-u.ac.jp

Abstract—We present a numerical study on the effect of laser light irradiation on the electronic transport through single layer graphene. We employed the wave packet quantum dynamics method to take into account the effect of laser light with circular polarization irradiated only through the finite channel region of graphene device. Our simulations have shown that the transmission through graphene can be switched off by irradiating the circularly polarized laser light, in a way consistent with the generation of dynamical band gap by the circularly polarized light predicted previously. It has also been suggested that the presence of irradiation induced remote valley away from the Dirac point importantly influences the current switching.

I. INTRODUCTION

Recent advances in research of graphene based electronics range widely from the replacement of conventional semiconductor technology (more Moore) to new functional devices and materials (more than Moore and beyond CMOS) [1]. From the view point of the replacement of conventional silicon technology, high electron mobility, high thermal conductivity, and mechanical flexibility of graphene are key driving force. The inherent zero band gap problem, a serious drawback for transistor application, can be resolved at least in principle by various mechanism, ranging from classical ideas such as graphene nanoribbons, bilayer graphene applied to vertical electric field, and interaction with the substrate, to new principle ideas such as the strain induced pseudo magnetic field [2], [3] and the laser induced dynamical band gap [4]. Such new principles provide not only as a tool to open the band gap but also as a new paradigm of graphene electronics such as valleytronics [5], [6] and topology electronics [7].

The idea of laser light irradiation was first studied theoretically in Ref. [8], where it was predicted that the linearly polarized light can induce the dynamical bandgap at away from the Dirac point and it can induce the photo current through the p-n junction. Subsequently the bandgap opening at the Dirac point was also predicted to be possible if the circularly polarized light is irradiated [4], [9], [10], [11], [12]. Stimulated by the understanding of bulk electronic properties of laser light irradiated graphene, electronic transport properties of laser light irradiated graphene have also been studied theoretically [10], [13], [14]. More recently the effect of circularly polarized laser light on the electronic conductivity in graphene was also studied based on the conventional Boltzmann equation [15]. The effect of photo irradiation on the transport through graphene nanoribbons has also been studied extensively [16], [17], [18].
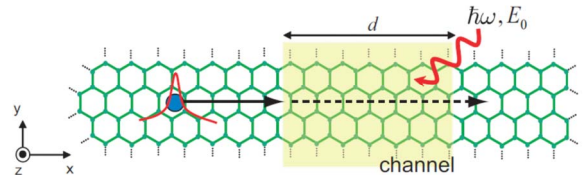

Fig. 1. (a) Schematic illustration of the device structure considered in this paper. Finite channel region with the length d along the x direction is irradiated by the laser field with the field intensity E_0 and angular frequency ω_0. Incident electron is represented by a Gaussian wave packet flows through graphene along the x direction.

These previous studies have provided various insights into the role of laser light in the transport through graphene. However, it has not been studied in detail on how the bandgap opening at the Dirac point induced by circularly polarized laser light influence the electronic current switching behavior in graphene. With such motivation, in this paper we study the transmission of electrons through graphene irradiated locally by circularly polarized light as illustrated in Fig. 1, by employing the real-time wave packet dynamics method.

II. THEORETICAL METHOD

A. Dynamical band structure of globally irradiated graphene

Let us first consider the effect of laser field irradiated globally to graphene. The electronic property of laser irradiated graphene near the Fermi energy can be described by the effective Dirac type Hamiltonian [19]

$$H(\boldsymbol{k}, t) = \hbar v_\mathrm{F} \boldsymbol{\sigma} \cdot \left(\boldsymbol{k} + \frac{e}{\hbar} \boldsymbol{A}(t) \right), \quad (1)$$

where v_F is the Fermi velocity and we assume a approximated value $v_\mathrm{F} = 10^6$ m/s, $\boldsymbol{\sigma} = (\sigma_x, \sigma_y)$ is the Pauli matrix, and $\boldsymbol{k} = (k_x, k_y)$ is the two-dimensional wave vector. The presence of the circularly polarized laser field is taken into account by the time-dependent vector potential as

$$\boldsymbol{A}(t) = \frac{E_0}{\omega_0} (\cos \omega_0 t \boldsymbol{e}_x + \sin \omega_0 t \boldsymbol{e}_y). \quad (2)$$

Then the time-dependent Schrödinger equation

$$i\hbar \frac{\partial}{\partial t} |\psi_{\boldsymbol{k}}(t)\rangle = H(\boldsymbol{k}, t) |\psi_{\boldsymbol{k}}(t)\rangle, \quad |\psi_{\boldsymbol{k}}(t)\rangle = \begin{pmatrix} \phi_{\boldsymbol{k}\mathrm{A}}(t) \\ \phi_{\boldsymbol{k}\mathrm{B}}(t) \end{pmatrix} \quad (3)$$

is solved for a given wavevector $\boldsymbol{k}$ with an apppropriate initial wavefunction $\phi_{\boldsymbol{k}\mathrm{A(B)}}(t=0)$ at the A(B) atom to obtain the time-series of the wavefunction $|\psi_{\boldsymbol{k}}(t)\rangle$. The obtained time-series of the wavefunction data is Fourier transformed with respect to time t to yield the spectral intensity $I(\boldsymbol{k},\omega)$ at a frequency ω. The spectral intensity $I(\boldsymbol{k},\omega)$ is used to plot the dynamical band structure in the next section.

B. Wave packet dynamics in locally photo-irradiated graphene

Calculation of electronic transmission through finite irradiated region requires real space analysis along the transport direction. For such purpose, in the Hamiltonian Eq.(1) the momentum operator along the x direction is replaced by the operator as $\hbar k_x \rightarrow -i\hbar\partial_x$, so that the Hamiltonian Eq.(1) now becomes

$$\hat{H} = v_F \left[\left(-i\hbar\partial_x + eA_x(x,t) \right) \sigma_x + \left(\hbar k_y + eA_y(x,t) \right) \sigma_y \right],$$
(4)

where $\boldsymbol{A}(x,t)$ is given by Eq. (2) in the irradiated channel region and zero otherwise. For the purpose of numerical calculations, moreover, x-derivative of the wavefunction is approximated by the finite-difference discretization with the grid spacing a, so that $\partial_x\psi(x)|_{x=x_l} \rightarrow [\psi_{l+1} - \psi_{l-1}]/2a$ with $\psi_l = \psi(x_l)$ and $\psi_{l\pm1} = \psi(x_l \pm a)$. Then the time-dependent Schrödinger equation can be written in the matrix form as

$$i\hbar\frac{\partial}{\partial t}\psi_{l\alpha}(k_y,t) = \sum_{m=-\infty}^{\infty} \sum_{m=\mathrm{A,B}} H_{lm,\alpha\beta}(k_y,t)\psi_{m\beta}(k_y,t),$$
(5)

where l and m are the grid index along the x direction, and α and β stand for A or B component given for each grid point l. The matrix element $H_{lm,\alpha\beta}(t)$ is given by

$$H_{lm,\alpha\beta}(t)$$
$$= \begin{cases} V_l, & (l=m, \alpha=\beta) \\ 2it_{\mathrm{hop}}\tilde{k}_y + 2t_{\mathrm{hop}}\left(A_x(t)+iA_y(t)\right)ea/\hbar, \\ & (l=m, \alpha=\mathrm{B}, \beta=\mathrm{A}) \\ -2it_{\mathrm{hop}}\tilde{k}_y + 2t_{\mathrm{hop}}\left(A_x(t)-iA_y(t)\right)ea/\hbar, \\ & (l=m, \alpha=\mathrm{A}, \beta=\mathrm{B}) \\ \pm it_{\mathrm{hop}}, & (l=m\pm1, \alpha=\beta) \\ 0, & \text{otherwise,} \end{cases}$$
(6)

where $t_{\mathrm{hop}} = \hbar v_F/2a$, $\tilde{k}_y = ak_y$, and $V_l = V(x_l)$. The time-dependent Schrödinger Eq. (5) can be solved once the initial wavefunction is given. In this study we assume the initial wavefunction given by the Gaussian wave packet

$$\psi(x,t=0) = \left(\pi\sigma^2\right)^{-1/4} \exp\left[-\frac{(x-x_0)^2}{2\sigma^2} + ik_0x \right]$$
(7)

where the broadening of the wavepacket is $\sigma = 20$ nm, and $k_0 = 1.52$ rad/nm corresponding to $\hbar v_F k_0 = 1.0$ eV. $\Delta k = 2/\sigma$, $\Delta E = \hbar v_F \Delta k = 0.0658$ eV. The initial position x_0 is assumed to be deep inside the left lead so that the initial wavepacket is not overlapped with the channel region. In order

to solve the time-dependent Schrödinger equations for large scale systems in real space, we employ the effecient numerical algorithm introduced in Ref. [20].
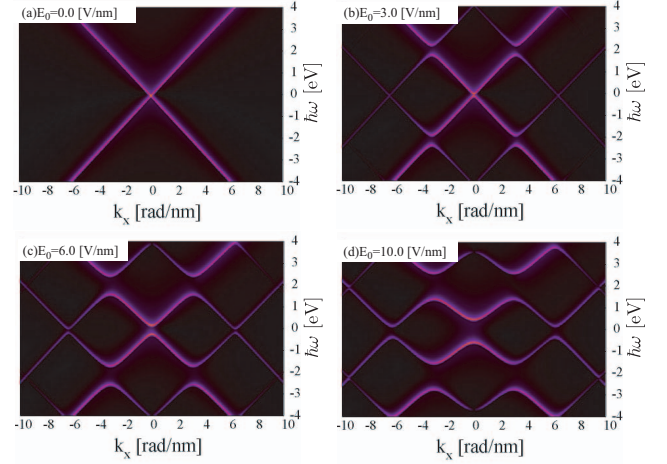

Fig. 2. Spectral intensity $I(\boldsymbol{k},\omega)$ of graphene irradiated globally by circularly polarized laser light with the field intensity E_0 and the angular frequency ω_0. Here k_y was set to zero, and the intensity $I(k_x,\omega)$ for the wavenumber k_x and the spectral frequency ω was visualized as the brightness of the colors (brighter color means the bigger spectral intensity). The frequency of the light was fixed as $\omega_0 = 6.28$ rad/fs, and results for various light intensities E_0 [(a) 0, (b) 3 V/nm, (c) 6 V/m, and (d) 10 V/nm] were compared.

III. RESULTS AND DISCUSSIONS

A. Dynamical band structure

In Fig. 2 we show the spectral intensity $I(\boldsymbol{k},\omega)$ obtained by using the method described in the last section. Here k_y was set to zero, and the intensity $I(k_x,\omega)$ for the wavenumber k_x and the frequency ω was visualized as the brightness of the colors (brighter color means the bigger spectral intensity). The frequency of the light was assumed to be $\omega_0 = 6.28$ rad/fs (wave length of $\lambda \sim 0.3$ μm), and results for various light intensities E_0 were compared. In this figure one can see that the dynamical band structure is modulated significantly due to the irradiation from the original Dirac linear dispersions, and the spectral gap (dynamical band gap) appears at around the Dirac point. It was also recognized that the dynamical band gap energy at the Dirac point increased as increasing the laser field intensity E_0. The dynamical bandgap at the Dirac point observed in Fig. 2 was in consistent with the analytically derived equation

$$E_{\mathrm{g}} = \sqrt{4\left(\frac{ev_F E_0}{\omega}\right)^2 + (\hbar\omega)^2} - \hbar\omega,$$
(8)

which was derived by using the Floquet theorem [4]. The existence of such this dynamically modulated band structure (Floquet-Bloch states) has been demonstrated experimentally on the surface of topological insulator [21], [22].

B. Transmission through laser irradiated region

1) Calculation model: Next we consider how the circularly polarized laser light irradiated locally to graphene influence the
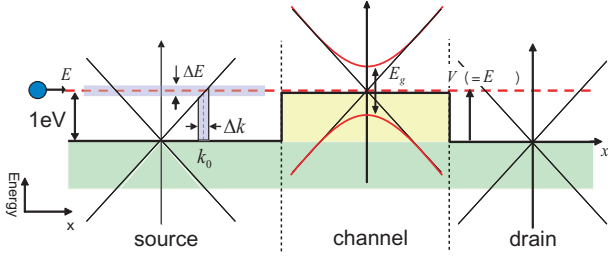
Fig. 3. Schematic illustration of the detailed device model structure assumed in the calculations. In the source and the drain regions the laser field is not irradiated and thus the band dispersion is linear and gapless. In the central channel region the circularly polarized light is irradiated and the finite band gap can be opened (red dispersion). Electron wave packet with the central energy $E = 1$ eV is injected from the source. In the central region, potential height $V = 1$ eV is assumed so that the electron with energy $E = 1$ eV passes through the middle of the band gap.

electronic transmission. To begin, in Fig. 3 we illustrate the detailed calculation model (also shown in Fig. 1) taking the energy in the vertical axis and x direction in the horizontal axis. The finite dynamical band gap E_g was illustrated in the central irradiated channel region (red dispersion), while the left and the right leads were not irradiated and thus the dispersions were gapless and linear. We also assumed the presence of static potential V only in the channel region. The energy of injected electron was fixed at $E = 1.0$ eV measured from the Dirac point in the leads, and the channel potential was $V = E = 1.0$ eV otherwise noted, so that the electron passes through the middle of the dynamical band gap in the channel region.

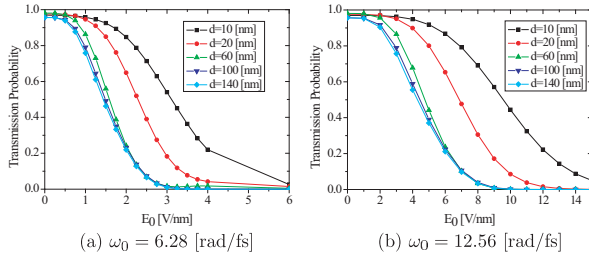(a) $\omega_0 = 6.28$ [rad/fs]   (b) $\omega_0 = 12.56$ [rad/fs]

Fig. 4. Transmission probability T as a function of the field intensity E_0 for various length d of the channel (laser irradiated) region and two different photo frequencies (a) $\omega_0 = 6.28$ and (b) 12.56 rad/fs are plotted.

2) Relation between electric transmission probability and field intensity E_0: In Fig. 4 we plotted the transmission probability T as a function of the field intensity E_0 for various length d of the channel (laser irradiated) region and two different photo frequencies $\omega_0 = 6.28$ and 12.56 rad/fs. Here we can see that the transmission probability decreased as increasing E_0 both for two frequencies. Such field induced switching was caused by the E_0 dependent dynamical bandgap at the Dirac point, made possible by the irradiation of circularly poralized light. An important observavtion in Fig. 4 is that the transmission probability drops off more abruptly (as a function of E_0) for longer channel length d, and the T-E_0 curve looks almost similarly when d is longer than 60 nm. It was also found that the field intensity E_0 required to switch-

off the transmission probability down to $T \sim 0$ was larger for larger frequency ω ($E_0 \simeq 3$ V/nm for $\omega = 6.28$ rad/fs and $E_0 \simeq 9$ V/nm for $\omega = 12.56$ rad/fs if d is long enough). Such threshold field $E_0^{(th)}$ can be determined by the dynamical bandgap E_g (calculated by Eq. (8) using E_0) satisfying $E_g = \Delta E \equiv \hbar v_F(2/\sigma)$, where the RHS is the energy width associated with the gaussian wavepacket width σ. For instance, for $\sigma = 20$ nm we obtained $\Delta E = 0.0658$ eV and then the values of E_0 satisfying $E_g = \Delta E$ were calculated as $E_0 \simeq 2.4$ V/nm for $\omega_0 = 2\pi$ rad/fs and $E_0 \simeq 6.77$ V/nm for $\omega_0 = 4\pi$ rad/fs, which were in consistent with the observed threshold field observed in Fig. 4 for enough long d. More gradual decrease of the transmission for shorter d can be interpreted to be caused by the tunneling through the bandgap.

The above mentioned behavior can be more clearly demonstrated in Fig. 5, where the transmission was plotted as a function of the bandgap E_g (not E_0) for various laser light frequency ω_0 and two different d. Here the value of E_g was calculated from the formula Eq. (8) using E_0 and ω_0. As demonstrated in Fig. 5, the obtained T-E_g curves behaved almost similarly independent of ω_0. In other words, once the channel length d is given, the transmission can be determined only through the bandgap E_g irrespective of the frequency ω_0 of the irradiated circularly polarized light.
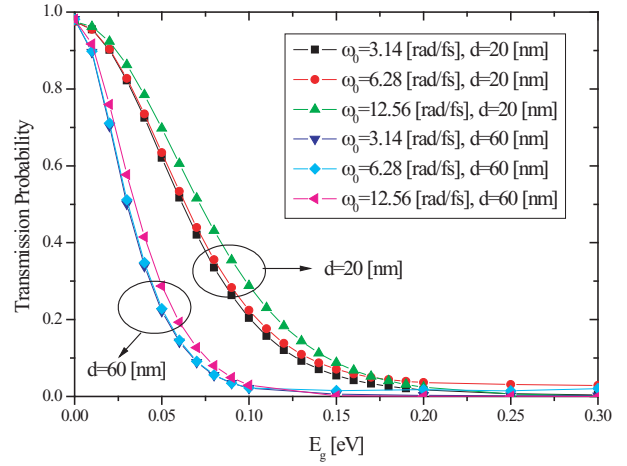

Fig. 5. Transmission probability as a function of the bandgap E_g for various laser light frequency ω_0 and two different values of d (20 nm and 60 nm). Value of E_g was calculated from the formula Eq. (8) using E_0 and ω_0.

3) Role of spectral intensity in the transmission probability controlled by potential barrier: So far we have assumed that the potential height V is equal to the electron energy E ($= 1.0$ eV), so that the electron energy (at the middle of its broadening) was always aligned with the middle of the laser induced dynamical band gap. Next we discuss how the transmission probability varies by changing the potential height V from $E = 1.0$ eV, while $E = 1.0$ eV is fixed. Such control of the barrier height can be realized experimentally by means of the static gate voltage. In the right panels of Figs. 6(a) and (b) we show the relationship between the applied

(a) E_0=10 V/nm, ω_0=6.28 rad/fs, d=60 nm

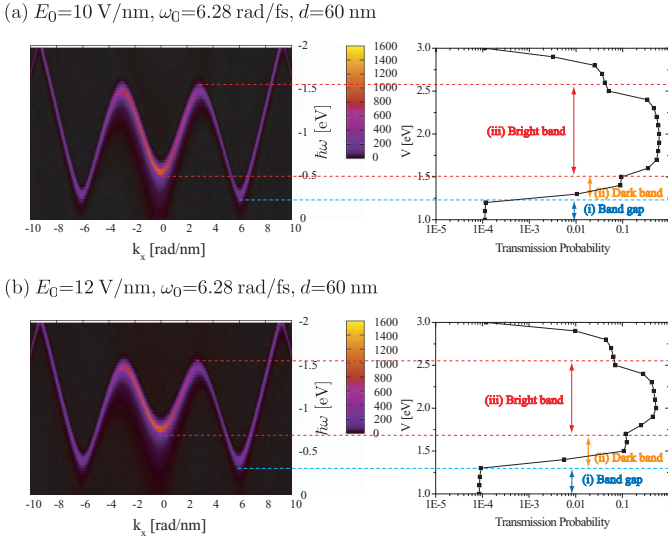(b) E_0=12 V/nm, ω_0=6.28 rad/fs, d=60 nm

Fig. 6. Right panel: Relationship between transmission probability and the potential height V in the central region. Left panel: Corresponding relation between the spectral intensity (brightness) and the spectral frequency (vertical axis). spectral intensity of dynamical band structure. Note that the vertical axis in the left panel is inverted to compare with the potential height in the right panel (see text for detail). Results for two different field intensities E_0 [(a) 10 V/nm and (b) 12 V/nm] were compared. Laser light frequency ω_0 and the length of the irradiated region d were fixed as 6.28 rad/fs and 60 nm, respectively.

potential V (vertical axis) and the transmission T (horizontal axis). When the potential V is changed from the original value $V = 1.0$ eV by v ($= 0 \sim 2$) in the positive (upward) direction, the dynamical band structure in the channel region is shifted upper in energy by v. Then the incoming electron energy $E = 1.0$ eV is arigned with the quasi-energy $\hbar\omega = -v$ eV in the original (unshifted) dynamical band structure plotted in the left panel. Then it is possible to analyze the transmission probability for the potential $V = 1.0 + v$ in the right panel in terms of the spectral intensity at the quasi-energy $\hbar\omega = -v$ in the left panel.

To proceed, it is important to recognize three different quasi-energy regimes in Fig. 6, *regime 1*: dynamical band gap regime ($|\hbar\omega| < 0.3$ eV), *regime 2*: dark band (lower spectral intensity) regime (0.3 eV $< |\hbar\omega| < 0.7$ eV), and *regime 3*: bright band (higher spectral intensity) regime ($0.7 < |\hbar\omega| < 1.5$ eV). As seen in Fig. 6, the transmission probability was smallest when the quasi energy was in the *regime 1* as expected. When the quasi energy was in the *regime 2*, importantly, non-negligible transmission ($T \sim 0.1$) was possible by electrons passing through the "dark band" located at around $k_x \simeq 6$ rad/nm away from the Dirac point. Finally in the *regime 3* the transmission was most significant as expected from the larger spectral intensity. It should be noted that electrons can be transmitted through the irradiated region not only using the "valley" at around the Dirac point, but also using the lower energy "remote valley" away from the Dirac point. Nevertheless, the spectral intensity of such "remote valley" was smaller compared with that of "Dirac valley" at around $k_x = 0$, and

thus the "Dirac valley" contributed most significantly to the transmission.

IV. Conclusion

In conclusion, we have presented a numerical study on the effect of circularly polarized laser light irradiation on the electronic transmission through single layer graphene, where we employed the wave packet dynamics to take into account the effect of laser field irradiated locally to the graphene. Our simulations have shown that the transmission through graphene can be significantly modulated by irradiating the laser field with the circular polarization, in a way consistent with the generation of bandgap by the circularly polarized light predicted previously. Moreover, the detailed analysis of the spectral intensity has suggested that the presence the remote valley induced by irradiation away from the Dirac point can influence the current switching importantly.

References

[1] K. S. Novoselov, V. I. Fal'ko, L. Colombo, P. R. Gellert, M. G. Schwab, and K. Kim, Nature, **490**, 192 (2012).
[2] V. M. Pereira and A. H. Castro Neto, Phys. Rev. Lett. **103**, 046801 (2009).
[3] S. Souma, M. Ueyama and M. Ogawa, Appl. Phys. Lett. **104** 213505 (2014).
[4] T. Oka, and H. Aoki, Phys. Rev. B **79**, 081406(R) (2009).
[5] T. L. Linnik, Phys. Rev. B **90**, 075406 (2014).
[6] A. Kundu, H. A. Fertig, and B. Seradjeh, Phys. Rev. Lett. **116**, 016802 (2016).
[7] G. Usaj, P. M. P. -Piskunow, L. E. F. F. Torres, and C. A. Balseiro, Phys. Rev. B **90**, 115423 (2014).
[8] S. V. Syzranov, M. V. Fistul, and K. B. Efetov, Phys. Rev. B **78**, 045407 (2008).
[9] O. V. Kibis, Phys. Rev. B **81**, 165433 (2010).
[10] H. L. Calvo, H. M. Pastawski, S. Roche, and L. E. F. Torres, Appl. Phys. Lett. **98**, 232103 (2011).
[11] Y. Zhou and M. W. Wu, Phys. Rev. B **83**, 245436 (2011).
[12] Phys. Rev. B **85**, 155449 (2012). M. Busl, G. Platero, and A. P. Jauho, Dynamical polarizability of graphene irradiated by circularly polarized ac electric fields
[13] C. Sinha and R. Biswas, Appl. Phys. Lett. **100**, 183107 (2012).
[14] R. Biswas and C. Sinha, J. Appl. Phys. **114**, 183706 (2013).
[15] K. Kristinsson, S. Kibis, O. V.and Morina, and I. A. Shelykh, Sci. Rep. **6**, 20082 (2016).
[16] C. G. Rocha, L. E. F. F Torres, and G. Cuniberti, Phys. Rev. B **81**, 115435 (2010).
[17] Z. Gu, H. A. Fertig, D. P. Arovas, and A. Auerbach, Phys. Rev. Lett **107**, 216601 (2011).
[18] H. L. Calvo, P. M. P.-Piskunow, S. Roche, and L. E. F. F. Torres, App. Phys. Lett., **101**, 253506 (2012).
[19] M. I. Katsnelson, K. S. Novoselov, and A. K. Geim, Nature Physics, **2**, 620 (2006).
[20] T. Tada, T. Yamamoto, and S. Watanabe, Theor. Chem. Acc. **130**, 775 (2011).
[21] Y. H. Wang, H. Steinberg, P. J.-Herrero, N. Gedik, Science **342**, 453 (2013).
[22] F. Mahmood, C. -K. Chan, Z. Alpichshev, D. Gardner, Y Lee, P. A. Lee and N. Gedik, Nature Physics **12**, 306 (2016).